

Learning Aggregations of Binary Activated Neural Networks with Probabilities over Representations

Louis Fortier-Dubois
Pascal Germain

Gaël Letarte
Université Laval

Benjamin Leblanc
François Laviotte

Abstract

Considering a probability distribution over parameters is known as an efficient strategy to learn a neural network with non-differentiable activation functions. We study the expectation of a probabilistic neural network as a predictor by itself, focusing on the aggregation of binary activated neural networks with normal distributions over real-valued weights. Our work leverages a recent analysis derived from the PAC-Bayesian framework that derives tight generalization bounds and learning procedures for the expected output value of such an aggregation, which is given by an analytical expression. While the combinatorial nature of the latter has been circumvented by approximations in previous works, we show that the exact computation remains tractable for deep but narrow neural networks, thanks to a dynamic programming approach. This leads us to a peculiar bound minimization learning algorithm for binary activated neural networks, where the forward pass propagates probabilities over representations instead of activation values. A stochastic counterpart of this new neural networks training scheme that scales to wider architectures is proposed.

1 INTRODUCTION

The computation graphs of deep neural networks (*a.k.a.* architectures) are challenging to analyze, due to their multiple composition of non-linearities [Ba and Caruana, 2014], overparametrization [Zhang et al., 2017] and highly non-convex learning objective [Dauphin et al.,

2014, Choromanska et al., 2015]. Studying simpler models seems a sensible strategy to gain insight on neural network behavior and state performance guarantees [*e.g.* Arora et al., 2019, Belkin et al., 2020]. Our work starts from one possible simplification, obtained by considering the binary activation function, meaning that each neuron outputs only one bit of information instead of the many bits needed to represent a real number. Note that the use of neural networks involving binary weights, with or without binary activation [Courbariaux et al., 2015, Hubara et al., 2016], have been suggested for reducing their resource consumption, and these may be especially useful in view of using a pre-trained network for forward propagation on embedded systems, but this is not our primary objective.

We study aggregations of binary activated networks with real-valued parameters. These are viewed as elementary pieces over which we consider a probability distribution. This is motivated by the recent analysis of Letarte et al. [2019], rooted in the PAC-Bayes theory [McAllester, 1999]: they propose a learning objective derived from a high-confidence generalization bound, and they empirically show that minimizing this objective provides a predictor with both tight and theoretically sound guarantees. They also derived an analytical expression for the expected output value of binary activated networks sampled from Gaussian distributions. Being differentiable, this expression enables gradient descent optimization, and is to be added to methods to train networks with non-differentiable activation functions [Williams, 1992, Bengio et al., 2013, Hubara et al., 2017]. However, in order to preserve valid PAC-Bayes guarantees and be able to train large neural networks, Letarte et al. [2019] relies on an approximation: neurons on the same layer all treat their inputs as if they were independent draws of the same probability distribution, when in fact all the inputs must correspond to the same draw. This recalls the *mean-field approximation* performed by Soudry et al. [2014] for learning binary activated networks in a Bayesian setting. Not only does this make the algorithm output values that are slightly straying from the true aggregation expec-

tation, it also fatally increases the PAC-Bayes bound for deeper architectures.

Our contribution overcomes this limitation : we show that it is possible to find the exact expectation of an aggregation of binary activated networks in time exponential in the width of the network, and linear in its depth, and present a stochastic version with sub-exponential time complexity regarding the network width. The originality of our proposed learning algorithm relies on the fact that it computes probabilities of occurrences of the hidden layer representations. Doing so, not only our algorithm allows us to obtain non-vacuous PAC-Bayes bounds for very deep binary activated networks, but reveals itself as an interesting prediction mechanism. Noteworthy, we show that once the parameters are optimized, the prediction on a new example is achievable with a time complexity that remains *constant* relatively to the network depth.

2 BACKGROUND AND NOTATION

We focus our study on the task of binary classification, using *binary activated multilayer* (BAM) neural networks, *i.e.*, networks where each neuron either outputs -1 or $+1$, using the sign function:

$$\text{sgn}(x) = \begin{cases} -1 & \text{if } x < 0, \\ +1 & \text{if } x \geq 0. \end{cases}$$

We suppose fully connected BAMs of $L \in \mathbb{N}^+$ layers of size $d_k \in \mathbb{N}^+$, $\forall k \in \{1, 2, \dots, L\}$, and inputs of size $d_0 \in \mathbb{N}^+$. We fix $d_L = 1$, whose output is the classification output of the whole network. We call L the *depth* of the network, d_k the *width* of the k^{th} layer, and $\max_{k \in \{1, 2, \dots, L\}} d_k$ the *width* of the network. The sequence $\langle d_k \rangle_{k=0}^L$ constitutes a (fully connected) *architecture*. Unlike in *binary* neural networks [*e.g.* Courbariaux et al., 2015], the parameters of a BAM are not constrained to be binary, but only activations are binary-valued. We thus have weights $\mathbf{W}_k \in \mathbb{R}^{d_k \times d_{k-1}}$ and biases $\mathbf{b}_k \in \mathbb{R}^{d_k}$, for $k \in \{1, 2, \dots, L\}$. That being said, in the remaining, the equations will be stated without loss of generality in terms of the weights \mathbf{W}_k only. Therefore, a BAM \mathcal{B} is totally defined by the tuple $\mathcal{B} := \langle \mathbf{W}_k \rangle_{k=1}^L$. See Fig. 1a for an example of architecture. The 0^{th} layer is the input layer, the 1^{st} one is the *leading* hidden layer, any k^{th} layer, with $1 < k < L$, is simply called a hidden layer and the L^{th} one is the output layer.

Following the premises of Letarte et al. [2019], we consider a generalization over BAMs, which we call an aggregation of BAMs.

Definition 1. An aggregation of BAMs with mean parameters $\mathcal{B}_M = \langle \mathbf{W}_k \rangle_{k=1}^L$, denoted $\mathcal{A}(\mathcal{B}_M)$, is given by

a Gaussian probability distribution over all parameters, centered in \mathcal{B}_M , with identity covariance matrix.

The BAM forward propagation process consists of computing the following function for an input $\mathbf{x} \in \mathbb{R}^{d_0}$, where sgn is defined element-wise:

$$F_{\mathcal{B}}(\mathbf{x}) = \text{sgn}(\mathbf{W}_L \text{sgn}(\mathbf{W}_{L-1} \text{sgn}(\dots \text{sgn}(\mathbf{W}_1 \mathbf{x}) \dots))).$$

In other words, the output of a BAM \mathcal{B} is $F_{\mathcal{B}}(\mathbf{x}) := F_{\mathcal{B}}^L(\mathbf{x})$, supposing the recursive equations

$$F_{\mathcal{B}}^k(\mathbf{x}) = \begin{cases} \text{sgn}(\mathbf{W}_1 \mathbf{x}) & \text{if } k = 1, \\ \text{sgn}(\mathbf{W}_k F_{\mathcal{B}}^{k-1}(\mathbf{x})) & \text{otherwise.} \end{cases}$$

On the other hand, the output of an *aggregation of BAMs* is the expected output of a BAM drawn from the parameters distribution:

$$F_{\mathcal{A}(\mathcal{B}_M)}(\mathbf{x}) = \mathbf{E}_{\mathcal{B} \sim \mathcal{A}(\mathcal{B}_M)} F_{\mathcal{B}}(\mathbf{x}). \quad (1)$$

Such aggregation of BAMs is our main object of study. Note that the forthcoming Section 4 is dedicated to a PAC-Bayesian treatment where $\mathcal{A}(\mathcal{B}_M)$ is considered as a *posterior distribution*. In line with the (PAC-)Bayesian literature, we call the single BAM network \mathcal{B}_M the *Maximum-A-Posteriori* (MAP) predictor.

3 THE AGGREGATION OUTPUT

We present a recursive formulation to compute the exact aggregation output, denoted $F_{\mathcal{A}(\mathcal{B}_M)}(\mathbf{x})$, which is differentiable end-to-end. The following formulation inherits from the analysis of Letarte et al. [2019], but is expressed in terms of the individual probabilities of representations for each layer.

First, given a *fixed* representation (*i.e.*, an input vector $\mathbf{a} \in \mathbb{R}^d$), the expected output of a single neuron with sign activation over an isotropic Gaussian distribution centered on weights $\mathbf{w} \in \mathbb{R}^d$ is

$$\mathbf{E}_{\mathbf{v} \sim \mathcal{N}(\mathbf{w}, \mathbf{I})} \text{sgn}(\mathbf{v} \cdot \mathbf{a}) = \text{erf}\left(\frac{\mathbf{w} \cdot \mathbf{a}}{\sqrt{2} \|\mathbf{a}\|}\right),$$

where $\text{erf}(x) = \frac{2}{\sqrt{\pi}} \int_0^x e^{-t^2} dt$ is the Gauss error function. However, as the input vector of a neuron relies on the distribution of weights on the previous layers, the representation itself is a random vector. A neuron outputs a value $s \in \{-1, 1\}$ with probability

$$\Pr(f_{\mathbf{w}}(\mathbf{a}) = s) = \frac{1}{2} + \frac{s}{2} \text{erf}\left(\frac{\mathbf{w} \cdot \mathbf{a}}{\sqrt{2} \|\mathbf{a}\|}\right). \quad (2)$$

Thus, the probability of observing a specific representation $\mathbf{s} = (\mathbf{s}^1, \dots, \mathbf{s}^{d_k}) \in R_k := \{-1, 1\}^{d_k}$ at layer k can

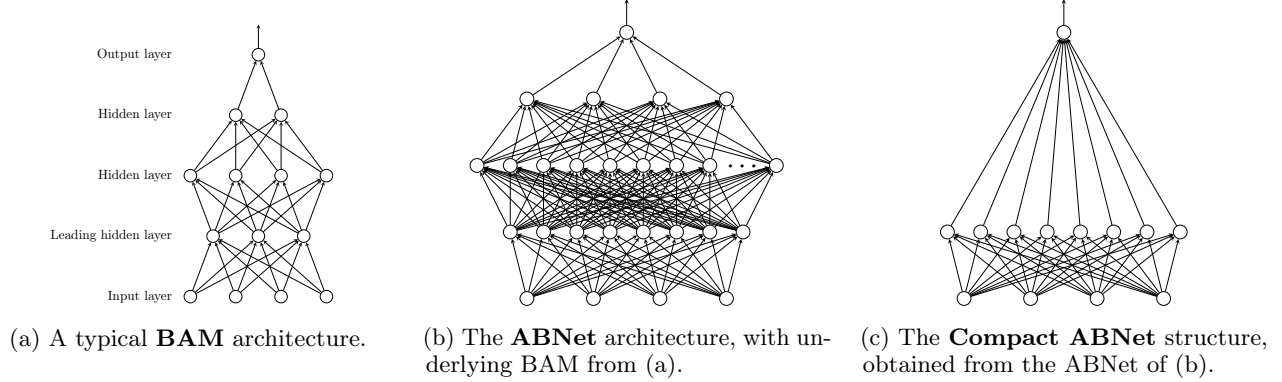


Figure 1: The BAM shown in (a) has depth $L = 4$, and widths $\langle d_k \rangle_{k=0}^4 = \langle 4, 3, 4, 2, 1 \rangle$. In (b), hidden layers have a width of 2^{d_k} (*i.e.*, one neuron per binary representation obtainable from a layer width of d_k in the underlying BAM). In (c), all hidden layers are merged, leaving a depth of 2 (as explained in Section 5).

be expressed in a recursive manner, having the events $a_k^s := F_{\mathcal{B}}^k(\mathbf{x}) = s$ and $a_{k-1}^{\bar{s}} := F_{\mathcal{B}}^{k-1}(\mathbf{x}) = \bar{s}$:

$$\Pr(a_k^s) = \begin{cases} \prod_{i=1}^{d_1} \left(\frac{1}{2} + \frac{s^i}{2} \operatorname{erf} \left(\frac{\mathbf{W}_1^i \cdot \mathbf{x}}{\sqrt{2} \|\mathbf{x}\|} \right) \right) & \text{if } k = 1, \\ \sum_{\bar{s} \in R_{k-1}} \Pr(a_k^s | a_{k-1}^{\bar{s}}) \Pr(a_{k-1}^{\bar{s}}) & \text{otherwise.} \end{cases}$$

The base case of the above recursion corresponds to the leading hidden layer (*i.e.*, $F_{\mathcal{B}}^1$). The probability of observing the representation $s \in R_1$ on this first hidden layer given an input \mathbf{x} amounts to be the product of the probability associated with the d_1 individual neuron values (Equation 2).

The general case corresponds to the subsequent hidden layers (*i.e.*, $F_{\mathcal{B}}^2, \dots, F_{\mathcal{B}}^L$). The probability of observing the representation $s \in R_k$ is decomposed into the sum of the $2^{d_{k-1}}$ probabilities of observing the representation $\bar{s} \in R_{k-1}$ on the previous hidden layer (obtained recursively) and the conditional probability (obtained from Equation (2), using the fact that $\|\bar{s}\|^2 = d_{k-1}$):

$$\Pr(a_k^s | a_{k-1}^{\bar{s}}) = \prod_{i=1}^{d_k} \left(\frac{1}{2} + \frac{s^i}{2} \operatorname{erf} \left(\frac{\mathbf{W}_k^i \cdot \bar{s}}{\sqrt{2d_{k-1}}} \right) \right).$$

Finally, assuming the output layer is only one neuron wide, the exact output of the aggregation can be computed with: $F_{\mathcal{A}(\mathcal{B}_M)}(\mathbf{x}) = \mathbf{E}_{\mathcal{B} \sim \mathcal{A}(\mathcal{B}_M)} F_{\mathcal{B}}(\mathbf{x}) = \Pr(F_{\mathcal{B}}^L(\mathbf{x})=1) - \Pr(F_{\mathcal{B}}^L(\mathbf{x})=-1)$.

By contrast, the proposed PBGNet algorithm of Letarte et al. [2019, Eq. (16)] computes $F_{PBG}^L(\mathbf{x})$ given the following equations (equivalent to the ones above only

when $L \leq 2$), with $c_i = \left(\frac{1}{2} + \frac{\bar{s}^i}{2} (F_{PBG}^k(\mathbf{x}))^i \right)$:

$$F_{PBG}^k(\mathbf{x}) = \begin{cases} \operatorname{erf} \left(\frac{\mathbf{W}_1 \cdot \mathbf{x}}{\sqrt{2} \|\mathbf{x}\|} \right) & \text{if } k = 1, \\ \sum_{\bar{s} \in R_{k-1}} \operatorname{erf} \left(\frac{\mathbf{W}_k \cdot \bar{s}}{\sqrt{2d_{k-1}}} \right) \prod_{i=1}^{d_k} c_i & \text{otherwise.} \end{cases}$$

This comes down to outputting at each layer only the expectation of the BAM representation given the expectation of the previous layer, instead of our complete probability distribution. Their method therefore deletes information at each layer since the expectation does not carry the correlation between each individual neuron output. This approximation recalls the mean-field one, on which the Bayesian analysis of binary activated networks of Soudry et al. [2014] relies. We avoid such approximations, and we compute $F_{\mathcal{A}(\mathcal{B}_M)}(\mathbf{x})$ by a dynamic programming approach, described next.

Dynamic program. Posing¹

$$\Psi_k = \left[\prod_{i=1}^{d_k} \left(\frac{1}{2} + \frac{s^i}{2} \operatorname{erf} \left(\frac{\mathbf{W}_k^i \cdot \bar{s}}{\sqrt{2d_{k-1}}} \right) \right) \right]_{s \in R_k, \bar{s} \in R_{k-1}}, \quad (3)$$

one can obtain straightforwardly the probability vector $\mathbf{P}_k = [\Pr(F_{\mathcal{B}}^k(\mathbf{x})=s)]_{s \in R_k} = \Psi_k \cdot \mathbf{P}_{k-1}$. Starting with

$$\mathbf{P}_1(\mathbf{x}) = \left[\prod_{i=1}^{d_1} \left(\frac{1}{2} + \frac{s^i}{2} \operatorname{erf} \left(\frac{\mathbf{W}_1^i \cdot \mathbf{x}}{\sqrt{2} \|\mathbf{x}\|} \right) \right) \right]_{s \in R_1}, \quad (4)$$

and computing \mathbf{P}_k for $k \in \{2, 3, \dots, L\}$ in ascending order, it is therefore possible to compute the exact expectation of a BAM $\mathcal{B} \sim \mathcal{A}$ in time exponential in \mathcal{B} 's width, but only linear in its depth.

The previous formulas lead to what stands as the forward propagation process of our new neural network,

¹Abusing notation a little, when writing $[g(\mathbf{s})]_{\mathbf{s} \in R}$ we assume all \mathbf{s} are taken in lexicographical order.

which we name *ABNet* for *Aggregation of Binary activated Networks* (see Algorithm 1 in Appendix A). From parameters \mathcal{B}_M , it computes $F_{\mathcal{A}(\mathcal{B}_M)}(\mathbf{x})$. The computation graph of ABNet is illustrated by Fig. 1b. The width of input and hidden layers $k < L$ are of exponential size 2^{d_k} relatively to the width d_k of the BAM networks it aggregates. Each layer of ABNet outputs a probability distribution over all possible configurations of the underlying BAM. The next layer then multiplies those probabilities by the conditional probabilities Ψ , which is just a reorganization of the weights and is totally independent of the input \mathbf{x} . As a result, ABNet applies only linear functions on hidden and output layers; an observation we discuss further in Section 5. Since every operation of ABNet is differentiable, we can use an automatic differentiation mechanism to efficiently compute the derivatives, then train the network via backpropagation and stochastic gradient descent.

Stochastic version. ABNet has many interesting theoretical properties, but the necessity of computing the probability of every combination of neuron outputs at a given layer makes it too cumbersome for practical applications. We propose a stochastic version of ABNet, which keeps its property of avoiding the mean field approximation while limiting the computation complexity with regard to the width to a quadratic one. This is achievable by picking a constant number n of representations R'_k uniformly from R_k at layer k , computing only the occurring probability of those n representations (replacing representation sets R_k by their uniformly drawn counterparts R'_k in Equations 3 and 4), and normalizing at each layer by dividing \mathbf{P}_k by $\sum_{\mathbf{s}_k \in R'_k} \mathbf{P}_k[\mathbf{s}_k]$ (see Algorithm 2 in Appendix A).

Complexity. Assuming every layer has the same width d at each layer, the complexity of PBGNet is $\mathcal{O}(L2^d d^2)$ (or $\mathcal{O}(Ln d^2)$ for its stochastic counterpart, with n samples), while the complexity of ABNet is $\mathcal{O}(L2^{2d} d^2)$ (or $\mathcal{O}(Ln^2 d^2)$ for the stochastic version). See Appendix B for an empirical study of computing times. A salient fact is that stochastic versions scale much better on wide architectures (Fig. 4).

4 BOUNDING AND OPTIMIZING THE GENERALIZATION LOSS

Initiated by McAllester [1999], the PAC-Bayes theory allows one to bound the generalization error of a learned predictor without requiring a validation set, under the sole assumption that data is sampled in an *iid* way from the unknown distribution \mathcal{D} . To be eligible for a PAC-Bayesian treatment, predictors must be expressed through a *posterior* probability distribution over a predefined class of *hypotheses*. Despite the fact that neural networks are not naturally defined as

such, many valuable analyses have been proposed by applying a PAC-Bayesian theory to stochastic variants of deterministic neural networks [Langford and Caruana, 2001, Dziugaite and Roy, 2018, Zhou et al., 2019, Pérez-Ortiz et al., 2020, Pitas, 2020] by considering perturbations (typically Gaussian distributed noise) on the weights. This strategy can be applied to any neural network topology and activation functions, but the generalization bounds do not apply to the underlying deterministic (non-perturbed) network.

By adopting the construction of Letarte et al. [2019] and designing our predictor *natively* as a distribution over simple BAM networks (Equation 1), the PAC-Bayesian bound applies to the output of ABNet. The forthcoming Theorem 2 provides high confidence upper bound for the *generalization loss* of a learned ABNet, defined as $\mathcal{L}_{\mathcal{D}}(F_{\mathcal{A}}) = \mathbf{E}_{(\mathbf{x}, y) \sim \mathcal{D}} \ell(F_{\mathcal{A}}(\mathbf{x}), y)$, where $\ell(y', y) = \frac{1}{2}(1 - yy') \in [0, 1]$ is the linear loss for the binary classification problem. The two main quantities involved in the computation of the bound are the *empirical* loss on the learning sample $S = \{(\mathbf{x}_i, y_i)\}_{i=1}^n \sim \mathcal{D}^n$,

$$\hat{\mathcal{L}}_S(F_{\mathcal{A}}) = \frac{1}{n} \sum_{i=1}^n \ell(F_{\mathcal{A}}(\mathbf{x}_i), y_i), \quad (5)$$

and the *Kullback-Leibler (KL)* divergence between the learned parameters (posterior distribution) $\mathcal{B} = \langle \mathbf{W}_k \rangle_{k=1}^L$ and a reference (prior distribution) $\mathcal{B}^p = \langle \mathbf{W}_k^p \rangle_{k=1}^L$ which is independent of the training data.² By using isotropic Gaussians for both the prior and the posterior, the KL divergence is easily obtained with

$$\text{KL}(\mathcal{B} \parallel \mathcal{B}^p) = \frac{1}{2} \sum_{k=1}^L \|\mathbf{W}_k - \mathbf{W}_k^p\|^2. \quad (6)$$

The PAC-Bayes theorem below is borrowed from Letarte et al. [2019], which itself is a variation from a seminal result from Catoni [2007], but has the major advantage to directly deal with the trade-off between the empirical loss and the KL divergence (*i.e.*, the value of C in Equation (7) is the one minimizing the bound).

Theorem 2. *Given a data independent prior distribution \mathcal{B}^p and $\delta \in (0, 1)$, with probability at least $1 - \delta$ over a realization of the learning sample $S \sim \mathcal{D}^n$, the following holds for all posterior \mathcal{B} :*

$$\mathcal{L}_{\mathcal{D}}(F_{\mathcal{A}}) \leq \inf_{C > 0} \left\{ \frac{1}{1-e^{-C}} \left(1 - \exp \left[-C \hat{\mathcal{L}}_S(F_{\mathcal{A}}) - \frac{1}{n} \left(\text{KL}(\mathcal{B} \parallel \mathcal{B}^p) + \ln \frac{2\sqrt{n}}{\delta} \right) \right] \right) \right\}. \quad (7)$$

A salient feature of the PAC-Bayesian bounds is that they are uniformly valid (with probability at least $1 - \delta$)

²Following Dziugaite and Roy [2018], Letarte et al. [2019], Pitas [2020], we chose an SGD random initialization as \mathcal{B}^p .

for the whole family of posterior. This is particularly suited for the design of a bound minimization algorithm, as the right-hand side of Equation (7) suggests an objective to minimize, and is providing a generalization guarantee even when the optimization procedure does not converge to a global minimum. Thus, we propose to train the ABNet architecture by minimizing the bound given in Theorem 2 by stochastic gradient descent. That is, the following objective is optimized according to parameters \mathcal{B} and $C > 0$, where $d = \ln \frac{2\sqrt{n}}{\delta}$:

$$\frac{1}{1-e^{-C}} \left(1 - \exp \left[-C \hat{\mathcal{L}}_S(F_{\mathcal{A}}) - \frac{\text{KL}(\mathcal{B} \parallel \mathcal{B}^p) + d}{n} \right] \right). \quad (8)$$

Although this objective is similar to the learning algorithm PBGNet [Letarte et al., 2019], the proposed ABNet objective differs in two noticeable ways for networks of depth $L > 2$:

- (1) The predictor output, and therefore the empirical loss of Equation (5), corresponds to the exact BAM expectation and is computed thanks to the forward propagation routine of ABNet, instead of the more classical computational graph of PBGNet.
- (2) The KL divergence of Equation (6), acting as a regularization term, does give the same penalty to weights of every layer in ABNet. In contrast, the corresponding term in PBGNet penalizes weights by a growing factor according to the layer depth.

5 COMPACTING THE ABNET

Recall from Section 3 that the aggregation output can be computed with the matrix product

$$F_{\mathcal{A}(\mathcal{B})}(\mathbf{x}) = [1, -1] \cdot (\Psi_L(\Psi_{L-1}(\dots \Psi_3(\Psi_2 \mathbf{P}_1(\mathbf{x})) \dots))),$$

with $\langle \Psi_k \rangle_{k=2}^L$ and $\mathbf{P}_1(\mathbf{x})$ computed from parameters $\mathcal{B} = \langle \mathbf{W}_k \rangle_{k=1}^L$ according to Equations (3) and (4). From this point of view, ABNet simply computes a linear function of the *leading hidden layer representation* $\mathbf{P}_1(\mathbf{x})$, highlighting a limitation of all binary (and discrete-valued) activated neural networks. Indeed, all matrices Ψ_k are solely based on the weights and do not rely on the input layer. Since there is no activation function between hidden layers, dot product associativity allows us to state the following.

Proposition 3. *The output of an aggregation of BAMs $\mathcal{A}(\mathcal{B})$, where $\mathcal{B} = \langle \mathbf{W}_k \rangle_{k=1}^L$, with leading hidden layer width d_1 , and other hidden layers of arbitrary width, can be obtained by forward propagating in a compact (with regard to depth) neural network having a leading hidden layer of width 2^{d_1} with erf activation and an output layer of width 1 with identity activation:*

$$F_{\mathcal{A}}(\mathbf{x}) = \mathbf{H} \cdot \mathbf{P}_1(\mathbf{x}), \quad (9)$$

where $\mathbf{P}_1(\mathbf{x})$ is a vector of 2^{d_1} elements defining a probability distribution on the outputs of the leading hidden layer of \mathcal{B} on \mathbf{x} , and $\mathbf{H} \in [-1, 1]^{2^{d_1}}$ is a vector giving the expected output of the rest of the network given the output of the first layer, such that

$$\mathbf{H} = [1, -1] \cdot \Psi_L \cdot \Psi_{L-1} \cdot \dots \cdot \Psi_3 \cdot \Psi_2. \quad (10)$$

Since only $\mathbf{P}_1(\mathbf{x})$ changes in function of \mathbf{x} , for fixed weights one can numerically precompute $\mathbf{H} := [h_{\mathbf{s}}]_{\mathbf{s} \in R_1}$ once and for all \mathbf{x} . In the underlying BAM this is analogous to precomputing the output for every representation outputted by the leading hidden layer. Every entry of \mathbf{H} is a real number between -1 and 1 since it represents an expectation on a BAM output. Therefore:

Corollary 4. *Notwithstanding the fact that the underlying BAM architecture can be arbitrarily deep, the aggregation output can always be expressed in the following shallow form, with $h_{\mathbf{s}} \in [-1, 1]$:*

$$F_{\mathcal{A}}(\mathbf{x}) = \sum_{\mathbf{s} \in R_1} h_{\mathbf{s}} \prod_{i=1}^{d_1} \left(\frac{1}{2} + \frac{\mathbf{s}^i}{2} \text{erf} \left(\frac{\mathbf{W}_1^i \cdot \mathbf{x}}{\sqrt{2} \|\mathbf{x}\|} \right) \right). \quad (11)$$

Thus, forward propagation of ABNet can be computed in time constant with regard to L .

We call the algorithm that computes Equation (11) the *Compact ABNet*. See Fig. 1c for a visual representation. Interestingly, the PAC-Bayes generalization bound of Theorem 2 is not obtainable directly from the Compact ABNet parameters. Therefore, our bound minimization algorithm requires the ABNet architecture. Noteworthy, our empirical experiments (Section 6, Fig. 3) show that training deeper ABNet can achieve better generalization than a shallower architecture, even when both share a Compact architecture of the same size. Compacting our stochastic version is also possible. Since the dot product must be executed on fixed R'_k 's, the drawn samples must be predetermined and remain the same at each inference; this leads to a very concise classifier which performs just as well as the last learned Stochastic ABNet. As can be seen in Fig. 5 from Appendix B, compact networks are much faster at inference time than their deep equivalent, as their complexity does not increase with depth.

Our original approach of propagating probabilities over representations is what brings the light on the compactability phenomenon. It is a well-known result that any function can be approximated to an arbitrary level of accuracy with a neural network having as few as one hidden layer, given that the layer is wide enough [Hornik et al., 1989]. It has also been shown that a shallow "student" network can learn to mimic a deep "teacher" network to reach the same performance level [Ba and Caruana, 2014]. However, typical neural networks do not allow such an explicit construction that

maps an initially (non-linear) deep structure to a shallow form. The result of Proposition 3 is a curiosity that is worth analyzing further. Remarkably, there is a clear dichotomy between the roles of $\mathbf{P}_1(\mathbf{x})$ and \mathbf{H} : the former transforms data points into a probability distribution over the leading hidden layer representations, whereas the latter gives the aggregation output for each of those representations. Put otherwise, the first layer serves as an embedding and the rest of the layers operate as a classifier. Fig. 2 illustrates the particularity of the prediction mechanism of ABNet.

The leading hidden layer. Equation (9) implies that the leading hidden layer defines regions in the input space. All subsequent hidden layers together express the output value of these regions. Fig. 2a shows how those regions divide the input space on the toy problem. Note that each region is associated with one of the four leading hidden layer binary representation.

Each neuron of the leading hidden layer of a BAM defines a hyperplane in the input space, where inputs on one side are mapped to -1 , and 1 on the other side. Considering all regions that are enclosed between the hyperplanes yields up to 2^{d_1} regions, corresponding to the 2^{d_1} output representations R_1 . Many of those regions may stray very far from the actual data. For example in Fig. 2a the region corresponding to representation $(1, -1)$ exists on the other side of where the two planes meet, which is far from any existing data³.

Additional hidden layers. The vector \mathbf{H} represents by extension a function from $\{-1, 1\}^{d_1}$ to $[-1, 1]$. Its role is to determine what sign should be outputted for each region defined by the leading hidden layer, with a confidence term. Its content is not arbitrary since it must be obtained from the weights of the subsequent hidden layers as in Equation (10). Depth therefore adds expressivity to BAM aggregations by allowing regions created by the leading hidden layer to output uncorrelated signs, with more or less confidence.

As illustrated by Figures 2c-d, taking the output of ABNet is not equivalent as taking the output of its associated MAP. For the same parameters, the aggregation allows more complex regions than BAMs, taking advantage that an input can belong to several regions, with certain probabilities. Indeed, there exist points \mathbf{x} and parameters \mathcal{B}_M for which $\text{sgn}(F_{\mathcal{A}(\mathcal{B}_M)}(\mathbf{x})) \neq F_{\mathcal{B}_M}(\mathbf{x})$. For instance, many incorrectly classified -1 data points in Fig. 2d fall within the correct region in Fig. 2c because ABNet can compensate the proximity to the

central $+1$ region with a lesser proximity with $two -1$ regions. It is therefore worthy to use the aggregation as a predictor by itself instead of its MAP, for its expressive power. Indeed, Zhu et al. [2019] observe that ensemble methods on binary neural networks confer stability with regard to input and parameter perturbations, which leads to better generalization.

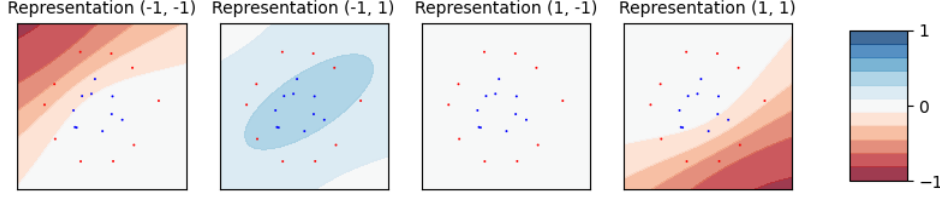
6 NUMERICAL EXPERIMENTS

We evaluated our proposed approach ABNet by following the experimental framework of Letarte et al. [2019], on the same six binary classification datasets: *ads* and *adult* from the UCI repository [Dua and Graff, 2017], along with four MNIST [LeCun et al., 1998] binary variants *mnistLH* (labels $\{0, 1, 2, 3, 4\}$ form the "Low" class, and $\{5, 6, 7, 8, 9\}$ the "High" class), *mnist17*, *mnist49* and *mnist56* (only examples labeled respectively 1&7, 4&9, and 5&6 are retained). As the exact versions of PBGNet and ABNet are limited by their exponential complexity regarding their width, we explored narrow network architectures (widths $d \in \{2, 4, 8\}$) and wider architectures (widths $d \in \{10, 50, 100\}$) accessible only to stochastic versions, all for 1 to 3 hidden layers.

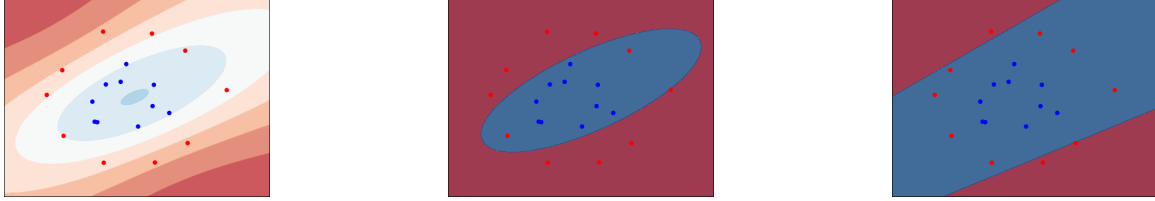
We first compare ABNet to its direct counterpart PBGNet [Letarte et al., 2019], both directly optimizing the PAC-Bayesian generalization bound during learning, with the prior distribution defined by the network weights random initialization. We also explore the minimization of the empirical loss with the variants ABNet_ℓ (Eq. 5) and PBGNet_ℓ , where 20% of the training data is used as a validation set for model selection.

Even if our work focuses on the learning of an aggregation of BAM, the optimization procedure of PBGNet and ABNet may be used to learn a single binary activated network, as a BAM itself is not learnable with standard gradient descent methods. We thus compare the *Maximum-A-Posteriori* (MAP) networks of both aggregated methods to three algorithms of the literature for learning neural networks with binary weights and/or activations: *Expectation Backpropagation* [Soudry et al., 2014] (EBP) with real-valued weights and binary activations, *Binarized Neural Network* [Hubara et al., 2016] (BNN) with both binary weights and activations, and *BinaryConnect* [Courbariaux et al., 2015] (BC) with binary weights but ReLU activations. Experiments involving EBP, BNN or BC are performed using fully connected networks, following the procedure used for ABNet_ℓ and PBGNet_ℓ . Results of the experiments are presented in Table 1. Note that standard deviations on each bound and train/test error are presented in Appendix C, along with results on BC and BNN (as these models don't rely on aggregation according to a posterior distribution).

³By considering the few most important region, one could potentially interpret ABNet predictions more easily than for classical neural networks. We consider this question as future work, and refer the reader to Montúfar et al. [2014] for a study of regions in the broader context of neural networks with continuous activations.



(a) For all \mathbf{x} , the probabilities of outputting a specific representation at the leading hidden layer, obtained from $\mathbf{P}_1(\mathbf{x})$, multiplied by the expected output for each of these regions, given by \mathbf{H} .



(b) The aggregation output $F_{\mathcal{A}(\mathcal{B}_M)}(\mathbf{x})$ for all \mathbf{x} , obtained by summing over all representations.

(c) Using ABNet as a classifier, one can simply use $\text{sgn}(F_{\mathcal{A}(\mathcal{B}_M)}(\mathbf{x}))$ as the prediction for an input \mathbf{x} .

(d) Using the BAM classifier from the MAP $F_{\mathcal{B}_M}(\mathbf{x})$, the decision boundary is less expressive.

Figure 2: Predictions of a learned ABNet and its underlying BAM with architecture $\langle 2, 2, 2, 1 \rangle$, *i.e.*, with two-dimensional inputs and two hidden layers, on a toy dataset.

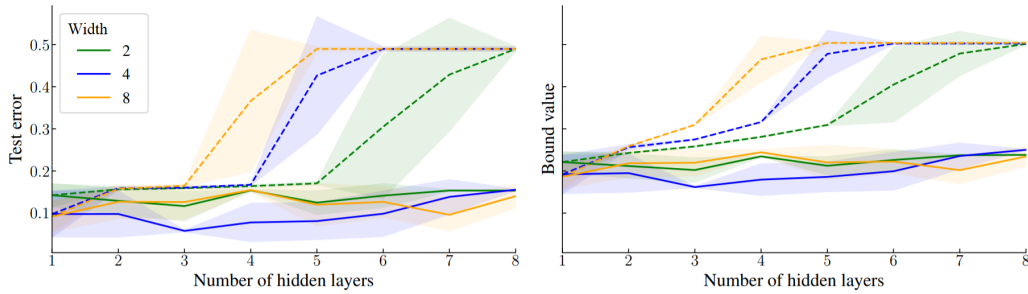


Figure 3: Impact of depth for **PBGNet (dashed)** and **ABNet (solid)** on test errors and bound values according to the width for mnistLH datasets. Results correspond to means and standard deviations over 5 repetitions.

Narrow architectures. The PAC-Bayesian inspired models with empirical loss minimization (PBGNet_ℓ and ABNet_ℓ) obtain competitive error rates (similar to the results achieved by BC using ReLU activations and binary weights, see Appendix C). However, the empirical loss minimization procedure lead to non-informative generalization bounds values. When considering the bound for optimization and model selection for PBGNet and ABNet, selected network architectures are smaller with usually a single hidden layer, as the objective function contains a regularization term on the weight values (see Eq. 8), and the error rates grow while bound values improve to a relevant level. We also notice that bound minimization algorithms are far less prone to *overfitting* than traditional optimization schemes, as their training errors are remarkably close to their testing errors (recall that PBGNet and ABNet are equivalent for one hidden layer). On the larger and harder dataset mnistLH, the narrow ABNet achieves a better error rate and bound value than PBGNet by selecting a

deeper architecture thanks to its less penalizing KL divergence regularization. On the performances of the MAP induced BAM networks, error rates are usually similar or slightly higher than the aggregated counterpart. Hence, these approaches can be considered as suitable algorithms to learn BAM networks.

Wide architectures. For all algorithms and most datasets, obtained results for wide and narrow binary neural networks are surprisingly similar. This reveals that constraining ABNet’s width to compute the exact aggregation output is not a major caveat. In particular, when one seeks tight PAC-Bayesian guarantees, lower complexity of narrow models should be favored. That being said, the proposed stochastic training for ABNet enables scaling to wider networks. While achieving most of the time comparable results to the stochastic PBGNet, the obtained risk on the large mnistLH dataset suggests that the approximation scheme of ABNet may not be as effective as the exact computation.

Table 1: Experiment results. On narrow architectures (left column), standard versions of PBGNet and ABNet are used, while their stochastic versions are used on wide architectures (right column). For each dataset and model, the best-performing set of parameters over the five repetitions is retained, and we show the number of hidden layers ($L-1$), hidden size (d), bound value and error rate on the train data (Error_S) and on the test data for the model (Error_T) and the associated *Maximum-A-Posteriori* BAM (MAP). See Appendix C for extended results.

Dataset	Model	Narrow architectures						Wide architectures					
		$L-1$	d	Bound	Error_S	Error_T	MAP	$L-1$	d	Bound	Error_S	Error_T	MAP
ads	PBGNet	3	2	0.192	0.140	0.141	0.141	3	10	0.213	0.140	0.141	0.141
	ABNet	3	2	0.192	0.140	0.141	0.141	2	10	0.216	0.140	0.141	0.141
	PBGNet ℓ	3	4	1.000	0.018	0.026	0.027	3	10	1.000	0.020	0.026	0.028
	ABNet ℓ	3	4	0.887	0.015	0.026	0.026	2	50	1.000	0.020	0.026	0.025
	EBP	2	2	–	0.003	0.040	0.054	3	10	–	0.005	0.035	0.049
adult	PBGNet	1	2	0.208	0.157	0.160	0.158	1	10	0.216	0.156	0.159	0.158
	ABNet	1	2	0.208	0.157	0.160	0.158	1	10	0.216	0.156	0.160	0.158
	PBGNet ℓ	3	4	0.723	0.135	0.149	0.156	2	10	0.360	0.146	0.151	0.164
	ABNet ℓ	3	4	0.780	0.132	0.149	0.150	3	10	0.541	0.143	0.151	0.151
	EBP	1	8	–	0.145	0.152	0.166	2	100	–	0.049	0.186	0.189
mnist17	PBGNet	1	2	0.036	0.005	0.006	0.006	1	10	0.041	0.005	0.006	0.006
	ABNet	1	2	0.036	0.005	0.006	0.006	1	10	0.041	0.005	0.006	0.006
	PBGNet ℓ	3	4	1.000	0.002	0.005	0.005	2	10	1.000	0.002	0.005	0.006
	ABNet ℓ	3	2	0.829	0.001	0.004	0.004	3	10	0.607	0.002	0.005	0.005
	EBP	1	2	–	0.000	0.006	0.006	2	10	–	0.000	0.005	0.005
mnist49	PBGNet	1	2	0.136	0.036	0.036	0.036	1	10	0.149	0.037	0.037	0.036
	ABNet	1	2	0.136	0.036	0.036	0.036	1	10	0.147	0.038	0.037	0.036
	PBGNet ℓ	2	4	1.000	0.008	0.020	0.020	1	50	0.992	0.004	0.012	0.012
	ABNet ℓ	3	8	1.000	0.004	0.017	0.017	3	10	1.000	0.024	0.029	0.027
	EBP	3	8	–	0.020	0.033	0.034	2	10	–	0.001	0.021	0.026
mnist56	PBGNet	1	2	0.084	0.021	0.023	0.023	1	10	0.090	0.023	0.025	0.024
	ABNet	1	2	0.084	0.021	0.023	0.023	1	10	0.090	0.023	0.025	0.024
	PBGNet ℓ	2	8	1.000	0.004	0.011	0.011	1	50	0.974	0.003	0.008	0.008
	ABNet ℓ	3	8	0.999	0.004	0.009	0.009	1	10	1.000	0.010	0.017	0.016
	EBP	3	8	–	0.001	0.010	0.015	2	10	–	0.000	0.019	0.021
mnistLH	PBGNet	1	8	0.186	0.091	0.092	0.093	1	10	0.167	0.058	0.059	0.060
	ABNet	3	4	0.162	0.056	0.058	0.059	2	10	0.187	0.087	0.088	0.087
	PBGNet ℓ	3	8	1.000	0.018	0.038	0.047	1	100	0.998	0.006	0.022	0.024
	ABNet ℓ	2	8	0.998	0.025	0.042	0.043	3	10	0.895	0.050	0.060	0.058
	EBP	3	8	–	0.016	0.043	0.082	1	100	–	0.001	0.027	0.032

Deep architectures. A key improvement of ABNet over PBGNet is the KL divergence computation which is not hindered by a growing factor penalizing the weights according to the network depth. This property should allow ABNet to learn deeper networks with tighter generalization bounds, which we investigated on the mnistLH dataset by extending the main experiment up to 8 hidden layers. Results are presented in Figure 3 where the difference of behavior between the models is clearly highlighted. For a small number of hidden layers, the performances are similar, but as the number of hidden layer grows, bound values for PBGNet sharply rise and test error rates degrade significantly. On the other hand, bound values are relatively stable for ABNet, indicating its potential to learn deep neural network architectures (the minimum bound is achieved for 3 hidden layers of width 4, which adequately indicates the best test error).

7 CONCLUSION

Many desirable properties stem from considering aggregations over binary activated networks with our algorithm ABNet. As PBGNet [Letarte et al., 2019], it gives a sensible way to optimize binary activated neural network parameters. It also provides tighter PAC-Bayes bounds on the generalization error of deep architectures, and leads to a surprisingly simple computation for finding an equivalent shallow network which emphasizes the role of each layer in a binary network. Extending the analysis to more complex prior and posterior distributions, such as Gaussian with diagonal covariance, should be explored in future works.

While we are building on the PAC-Bayes analysis of Letarte et al. [2019], our learning algorithm, and the analysis of the dichotomy between the first layers versus the others, are completely new. We believe the latter

is a powerful tool for understanding the expressivity conferred by a network’s architecture, which could enhance our understanding of the role of depth in neural networks, pursuing the work of Le Roux and Bengio [2010], Szymanski and McCane [2012] and Kidger and Lyons [2020], but in the context of model aggregation.

Societal Impact. When machine learning algorithms are deployed in the real world, ethical concerns must be considered. It is hazardous to use them in automated decision systems that might affect the welfare of individuals. The same applies to our algorithm; however, our focus on interpretability and certifiability is in line with the objective of attenuating those concerns.

References

Sanjeev Arora, Nadav Cohen, Noah Golowich, and Wei Hu. A convergence analysis of gradient descent for deep linear neural networks. In *ICLR*, 2019.

Jimmy Ba and Rich Caruana. Do deep nets really need to be deep? In *NIPS*, pages 2654–2662, 2014.

Mikhail Belkin, Daniel Hsu, and Ji Xu. Two models of double descent for weak features. *SIAM J. Math. Data Sci.*, 2(4):1167–1180, 2020.

Yoshua Bengio, Nicholas Léonard, and Aaron C. Courville. Estimating or propagating gradients through stochastic neurons for conditional computation. *CoRR*, abs/1308.3432, 2013.

Olivier Catoni. *PAC-Bayesian supervised classification: the thermodynamics of statistical learning*, volume 56. Inst. of Mathematical Statistic, 2007.

Anna Choromanska, Mikael Henaff, Michaël Mathieu, Gérard Ben Arous, and Yann LeCun. The loss surfaces of multilayer networks. In *AISTATS*, volume 38, 2015.

Matthieu Courbariaux, Yoshua Bengio, and Jean-Pierre David. Binaryconnect: Training deep neural networks with binary weights during propagations. In *NIPS*, pages 3123–3131, 2015.

Yann N. Dauphin, Razvan Pascanu, Çaglar Gülcehre, KyungHyun Cho, Surya Ganguli, and Yoshua Bengio. Identifying and attacking the saddle point problem in high-dimensional non-convex optimization. In *NIPS*, pages 2933–2941, 2014.

Dheeru Dua and Casey Graff. UCI machine learning repository, 2017. URL <http://archive.ics.uci.edu/ml>.

Gintare Karolina Dziugaite and Daniel M. Roy. Data-dependent PAC-Bayes priors via differential privacy. In *NeurIPS*, pages 8440–8450, 2018.

Kurt Hornik, Maxwell Stinchcombe, and Halbert White. Multilayer feedforward networks are universal approximators. *Neural networks*, 2(5):359–366, 1989.

Itay Hubara, Matthieu Courbariaux, Daniel Soudry, Ran El-Yaniv, and Yoshua Bengio. Binarized neural networks. In *NIPS*, 2016.

Itay Hubara, Matthieu Courbariaux, Daniel Soudry, Ran El-Yaniv, and Yoshua Bengio. Quantized neural networks: Training neural networks with low precision weights and activations. *JMLR*, 18(1):6869–6898, 2017.

Patrick Kidger and Terry J. Lyons. Universal approximation with deep narrow networks. In *COLT*, volume 125, pages 2306–2327, 2020.

Diederik P Kingma and Jimmy Ba. Adam: A method for stochastic optimization. In *ICLR*, 2015.

John Langford and Rich Caruana. (Not) bounding the true error. In *NIPS*, pages 809–816, 2001.

Nicolas Le Roux and Yoshua Bengio. Deep belief networks are compact universal approximators. *Neural computation*, 22(8):2192–2207, 2010.

Yann LeCun, Léon Bottou, Yoshua Bengio, and Patrick Haffner. Gradient-based learning applied to document recognition. *Proceedings of the IEEE*, 86(11):2278–2324, 1998.

Gaël Letarte, Pascal Germain, Benjamin Guedj, and François Laviolette. Dichotomize and generalize: Pac-bayesian binary activated deep neural networks. In *NeurIPS*, pages 6869–6879, 2019.

David McAllester. Some PAC-Bayesian theorems. *Machine Learning*, 37(3):355–363, 1999.

Guido F. Montúfar, Razvan Pascanu, KyungHyun Cho, and Yoshua Bengio. On the number of linear regions of deep neural networks. In *NIPS*, pages 2924–2932, 2014.

María Pérez-Ortiz, Omar Rivasplata, John Shawe-Taylor, and Csaba Szepesvári. Tighter risk certificates for neural networks. *CoRR*, abs/2007.12911, 2020.

Konstantinos Pitas. Dissecting non-vacuous generalization bounds based on the mean-field approximation. In *ICML*, 2020.

Daniel Soudry, Itay Hubara, and Ron Meir. Expectation backpropagation: Parameter-free training of multilayer neural networks with continuous or discrete weights. In *NIPS*, 2014.

Lech Szymanski and Brendan McCane. Deep, super-narrow neural network is a universal classifier. In *IJCNN*, pages 1–8. IEEE, 2012.

Ronald J. Williams. Simple statistical gradient-following algorithms for connectionist reinforcement learning. *Machine Learning*, 8(3):229–256, May 1992.

Chiyuan Zhang, Samy Bengio, Moritz Hardt, Benjamin Recht, and Oriol Vinyals. Understanding deep

learning requires rethinking generalization. In *ICLR*, 2017.

Wenda Zhou, Victor Veitch, Morgane Austern, Ryan P. Adams, and Peter Orbanz. Non-vacuous generalization bounds at the imagenet scale: a PAC-bayesian compression approach. In *ICLR*, 2019.

Shilin Zhu, Xin Dong, and Hao Su. Binary ensemble neural network: More bits per network or more networks per bit? In *CVPR*, pages 4923–4932, 2019.

A ALGORITHMS

We provide a detailed view on the forward propagation algorithms of ABNet and its stochastic counterpart, presented in Section 3. We use $R' \sim \mathcal{U}_n(R)$ to denote that R' consists of n draws (with replacement) from a uniform distribution on R .

Algorithm 1 ABNet

Require: $\mathbf{x} \in \mathbb{R}^{d_0}$ and $\mathcal{B}_M = \langle \mathbf{W}_k \rangle_{k=1}^L$, with $\mathbf{W}_k \in \mathbb{R}^{d_{k-1} \times d_k} \forall 1 \leq k \leq L$

- 1: $\mathbf{P} \leftarrow \left[\prod_{i=1}^{d_1} \left(\frac{1}{2} + \frac{\mathbf{s}_1^i}{2} \operatorname{erf}\left(\frac{\mathbf{W}_1^i \cdot \mathbf{x}}{\sqrt{2} \|\mathbf{x}\|}\right) \right) \right]_{\mathbf{s}_1 \in R_1}$
- 2: for $k \in \{2, \dots, L\}$ do
- 3: $\Psi = \left[\prod_{i=1}^{d_k} \left(\frac{1}{2} + \frac{\mathbf{s}_k^i}{2} \operatorname{erf}\left(\frac{\mathbf{W}_k^i \cdot \mathbf{s}_{k-1}}{\sqrt{2} d_{k-1}}\right) \right) \right]_{\mathbf{s}_k \in R_k, \mathbf{s}_{k-1} \in R_{k-1}}$
- 4: $\mathbf{P} \leftarrow \Psi \cdot \mathbf{P}$
- 5: return $[1, -1] \cdot \mathbf{P}$

Algorithm 2 Stochastic ABNet

Require: $\mathbf{x} \in \mathbb{R}^{d_0}$, $n \in \mathbb{N}$ and $\mathcal{B}_M = \langle \mathbf{W}_k \rangle_{k=1}^L$, with $\mathbf{W}_k \in \mathbb{R}^{d_{k-1} \times d_k} \forall 1 \leq k \leq L$

- 1: $R'_1 \sim \mathcal{U}_n(R_1)$
- 2: $\mathbf{P} \leftarrow \left[\prod_{i=1}^{d_1} \left(\frac{1}{2} + \frac{\mathbf{s}_1^i}{2} \operatorname{erf}\left(\frac{\mathbf{W}_1^i \cdot \mathbf{x}}{\sqrt{2} \|\mathbf{x}\|}\right) \right) \right]_{\mathbf{s}_1 \in R'_1}$
- 3: $\mathbf{P} \leftarrow \frac{\mathbf{P}}{\sum_{\mathbf{s}_1 \in R'_1} \mathbf{P}[\mathbf{s}_1]}$
- 4: for $k \in \{2, \dots, L\}$ do
- 5: $R'_k \sim \mathcal{U}_n(R_k)$
- 6: $\Psi = \left[\prod_{i=1}^{d_k} \left(\frac{1}{2} + \frac{\mathbf{s}_k^i}{2} \operatorname{erf}\left(\frac{\mathbf{W}_k^i \cdot \mathbf{s}_{k-1}}{\sqrt{2} d_{k-1}}\right) \right) \right]_{\mathbf{s}_k \in R'_k, \mathbf{s}_{k-1} \in R'_{k-1}}$
- 7: $\mathbf{P} \leftarrow \Psi \cdot \mathbf{P}$
- 8: $\mathbf{P} \leftarrow \frac{\mathbf{P}}{\sum_{\mathbf{s}_k \in R'_k} \mathbf{P}[\mathbf{s}_k]}$
- 9: return $\sum_{\mathbf{s}_L \in R'_L} \mathbf{s}_L \mathbf{P}[\mathbf{s}_L]$

B COMPUTATION TIME

All experiments were performed on NVIDIA GPUs GeForce RTX 2080 Ti. We present an empirical study of computation time needed by our four algorithms (ABNet, Stochastic ABNet, Compact ABNet and Compact stochastic ABNet) and by the benchmark PBGNet (and its stochastic version) in Figures 4 and 5.

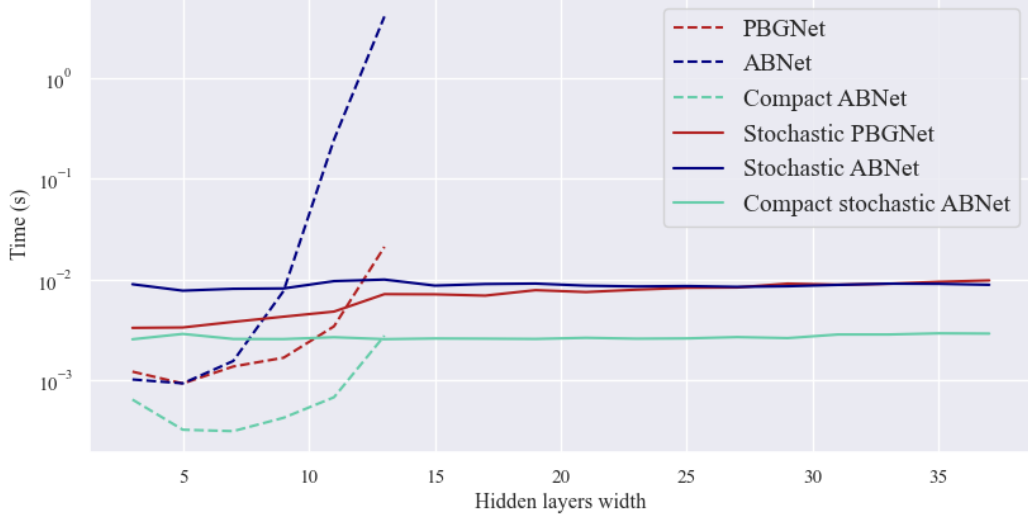


Figure 4: Time needed (in seconds) for the forward propagation of our four ABNet versions and the two versions of the PBGNet benchmark, all with 6 hidden layers and with 100 samples for stochastic versions. Computations were executed on a batch of 32 examples of the Ads dataset, averaged on 100 repetitions. Of note, the memory requirements of our (non-stochastic) PBGNet and ABNet implementations exceed the available resources for layer widths greater than 13.

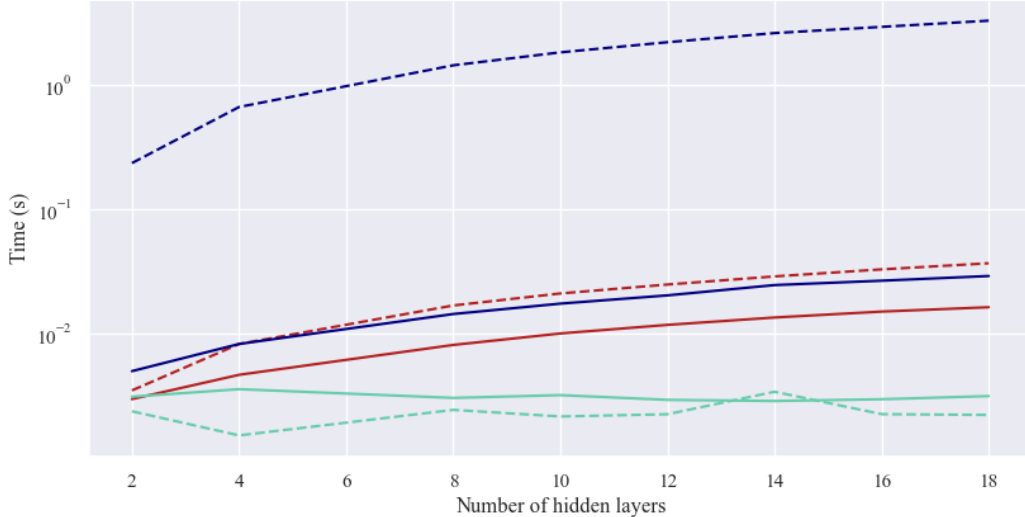


Figure 5: Time needed (in seconds) for the forward propagation of our four ABNet versions and the two versions of the PBGNet benchmark, all with width $d_k = 12$ for $1 \leq k < L$, and with 100 samples for stochastic versions. Computations were executed on a batch of 32 examples of the Ads dataset, averaged on 100 repetitions. See Figure 4 for the legend.

C DETAILED EXPERIMENTAL RESULTS

Tables 2 and 3 present complete results for the experiments of Table 1, respectively for narrow and wide architectures. Table 4 presents details about selected hyperparameters on stochastic PBGNet and ABNet. The source code of our experiments will be released with the paper publication.

Table 2: Extended experiment results with standard deviation on narrow architectures (with PBGNet and ABNet *exact* versions) on 5 repetitions for selected models: number of hidden layers ($L-1$), width (d), bound value and error rate on both train (Error_S) and test (Error_T) data and the associated *Maximum-A-Posteriori* BAM (MAP).

Dataset	Model	$L-1$	d	Bound	Error _S	Error _T	MAP
ads	PBGNet	3	2	0.192 ± 0.004	0.140 ± 0.004	0.141 ± 0.012	0.141 ± 0.012
	ABNet	3	2	0.192 ± 0.004	0.140 ± 0.004	0.141 ± 0.012	0.141 ± 0.012
	PBGNet ℓ	3	4	1.000 ± 0.001	0.018 ± 0.005	0.026 ± 0.004	0.027 ± 0.004
	ABNet ℓ	3	4	0.887 ± 0.064	0.015 ± 0.003	0.026 ± 0.003	0.026 ± 0.003
	EBP	2	2	—	0.003 ± 0.002	0.040 ± 0.008	0.054 ± 0.006
	BC	1	4	—	0.025 ± 0.005	0.031 ± 0.004	0.031 ± 0.004
	BNN	1	8	—	0.037 ± 0.002	0.038 ± 0.004	0.038 ± 0.004
adult	PBGNet	1	2	0.208 ± 0.001	0.157 ± 0.001	0.160 ± 0.003	0.158 ± 0.003
	ABNet	1	2	0.208 ± 0.001	0.157 ± 0.001	0.160 ± 0.003	0.158 ± 0.003
	PBGNet ℓ	3	4	0.723 ± 0.031	0.135 ± 0.001	0.149 ± 0.002	0.156 ± 0.002
	ABNet ℓ	3	4	0.780 ± 0.138	0.132 ± 0.005	0.149 ± 0.003	0.150 ± 0.003
	EBP	1	8	—	0.145 ± 0.002	0.152 ± 0.003	0.166 ± 0.005
	BC	1	8	—	0.142 ± 0.002	0.151 ± 0.002	0.151 ± 0.002
	BNN	1	2	—	0.180 ± 0.016	0.182 ± 0.017	0.182 ± 0.017
mnist17	PBGNet	1	2	0.036 ± 0.000	0.005 ± 0.000	0.006 ± 0.001	0.006 ± 0.001
	ABNet	1	2	0.036 ± 0.000	0.005 ± 0.000	0.006 ± 0.001	0.006 ± 0.001
	PBGNet ℓ	3	4	1.000 ± 0.000	0.002 ± 0.001	0.005 ± 0.001	0.005 ± 0.001
	ABNet ℓ	3	2	0.829 ± 0.078	0.001 ± 0.001	0.004 ± 0.001	0.004 ± 0.001
	EBP	1	2	—	0.000 ± 0.001	0.006 ± 0.001	0.006 ± 0.001
	BC	2	4	—	0.004 ± 0.000	0.010 ± 0.002	0.010 ± 0.002
	BNN	1	8	—	0.003 ± 0.001	0.008 ± 0.001	0.008 ± 0.001
mnist49	PBGNet	1	2	0.136 ± 0.002	0.036 ± 0.001	0.036 ± 0.004	0.036 ± 0.004
	ABNet	1	2	0.136 ± 0.002	0.036 ± 0.001	0.036 ± 0.004	0.036 ± 0.004
	PBGNet ℓ	2	4	1.000 ± 0.000	0.008 ± 0.003	0.020 ± 0.004	0.020 ± 0.004
	ABNet ℓ	3	8	1.000 ± 0.000	0.004 ± 0.002	0.017 ± 0.003	0.017 ± 0.003
	EBP	3	8	—	0.020 ± 0.003	0.033 ± 0.003	0.034 ± 0.004
	BC	2	8	—	0.007 ± 0.002	0.016 ± 0.002	0.016 ± 0.002
	BNN	1	2	—	0.030 ± 0.006	0.037 ± 0.003	0.037 ± 0.003
mnist56	PBGNet	1	2	0.084 ± 0.001	0.021 ± 0.003	0.023 ± 0.006	0.023 ± 0.005
	ABNet	1	2	0.084 ± 0.001	0.021 ± 0.003	0.023 ± 0.006	0.023 ± 0.005
	PBGNet ℓ	2	8	1.000 ± 0.000	0.004 ± 0.001	0.011 ± 0.003	0.011 ± 0.003
	ABNet ℓ	3	8	0.999 ± 0.001	0.004 ± 0.002	0.009 ± 0.002	0.009 ± 0.002
	EBP	3	8	—	0.001 ± 0.002	0.010 ± 0.004	0.015 ± 0.004
	BC	1	8	—	0.002 ± 0.001	0.009 ± 0.004	0.009 ± 0.004
	BNN	1	8	—	0.013 ± 0.003	0.023 ± 0.003	0.023 ± 0.003
mnistLH	PBGNet	1	8	0.186 ± 0.028	0.091 ± 0.037	0.092 ± 0.036	0.093 ± 0.036
	ABNet	3	4	0.162 ± 0.001	0.056 ± 0.001	0.058 ± 0.002	0.059 ± 0.002
	PBGNet ℓ	3	8	1.000 ± 0.000	0.018 ± 0.003	0.038 ± 0.002	0.047 ± 0.002
	ABNet ℓ	2	8	0.998 ± 0.003	0.025 ± 0.008	0.042 ± 0.006	0.043 ± 0.006
	EBP	3	8	—	0.016 ± 0.002	0.043 ± 0.002	0.082 ± 0.005
	BC	2	8	—	0.023 ± 0.002	0.035 ± 0.001	0.035 ± 0.001
	BNN	1	2	—	0.123 ± 0.005	0.133 ± 0.004	0.133 ± 0.004

All experiments were repeated with 5 different random train/test dataset splits and weights initializations. Networks parameters are optimized using Adam [Kingma and Ba, 2015] for the following learning rate values: $\{0.1, 0.01, 0.001, 0.0001\}$. Training is performed for 100 epochs with early stopping after 20 epochs without improvement. Note that for both BC and BNN algorithms, the Error_T and MAP columns share the same results, as these models don't rely on aggregation.

Table 3: Extended experiment results with standard deviation on wide architectures (with PBGNet and ABNet *stochastic* versions) over the 5 repetitions for selected models: number of hidden layers ($L-1$), width (d), bound value and error rate on the train data (Error_S) and on the test data for the model (Error_T) and the associated *Maximum-A-Posteriori* BAM (MAP).

Dataset	Model	$L-1$	d	Bound	Error_S	Error_T	MAP
ads	PBGNet	3	10	0.213 ± 0.004	0.140 ± 0.003	0.141 ± 0.010	0.141 ± 0.010
	ABNet	2	10	0.216 ± 0.004	0.140 ± 0.003	0.141 ± 0.010	0.141 ± 0.010
	PBGNet ℓ	3	10	1.000 ± 0.000	0.020 ± 0.003	0.026 ± 0.006	0.028 ± 0.003
	ABNet ℓ	2	50	1.000 ± 0.000	0.020 ± 0.005	0.026 ± 0.005	0.025 ± 0.004
	EBP	3	10	—	0.005 ± 0.002	0.035 ± 0.006	0.049 ± 0.008
	BC	1	10	—	0.021 ± 0.005	0.032 ± 0.005	0.032 ± 0.005
	BNN	1	100	—	0.029 ± 0.004	0.032 ± 0.005	0.032 ± 0.005
adult	PBGNet	1	10	0.216 ± 0.001	0.156 ± 0.001	0.159 ± 0.002	0.158 ± 0.002
	ABNet	1	10	0.216 ± 0.000	0.156 ± 0.001	0.160 ± 0.002	0.158 ± 0.002
	PBGNet ℓ	2	10	0.360 ± 0.004	0.146 ± 0.001	0.151 ± 0.002	0.164 ± 0.000
	ABNet ℓ	3	10	0.541 ± 0.033	0.143 ± 0.001	0.151 ± 0.002	0.151 ± 0.002
	EBP	2	100	—	0.049 ± 0.002	0.186 ± 0.001	0.189 ± 0.003
	BC	1	50	—	0.160 ± 0.003	0.164 ± 0.001	0.164 ± 0.001
	BNN	1	100	—	0.157 ± 0.002	0.165 ± 0.002	0.165 ± 0.002
mnist17	PBGNet	1	10	0.041 ± 0.000	0.005 ± 0.000	0.006 ± 0.001	0.006 ± 0.001
	ABNet	1	10	0.041 ± 0.000	0.005 ± 0.000	0.006 ± 0.001	0.006 ± 0.001
	PBGNet ℓ	2	10	1.000 ± 0.000	0.002 ± 0.001	0.005 ± 0.001	0.006 ± 0.001
	ABNet ℓ	3	10	0.607 ± 0.084	0.002 ± 0.000	0.005 ± 0.001	0.005 ± 0.001
	EBP	2	10	—	0.000 ± 0.000	0.005 ± 0.000	0.005 ± 0.001
	BC	3	50	—	0.003 ± 0.001	0.006 ± 0.001	0.006 ± 0.001
	BNN	1	100	—	0.004 ± 0.001	0.007 ± 0.001	0.007 ± 0.001
mnist49	PBGNet	1	10	0.149 ± 0.007	0.037 ± 0.001	0.037 ± 0.004	0.036 ± 0.004
	ABNet	1	10	0.147 ± 0.007	0.038 ± 0.001	0.037 ± 0.004	0.036 ± 0.004
	PBGNet ℓ	1	50	0.992 ± 0.001	0.004 ± 0.000	0.012 ± 0.003	0.012 ± 0.003
	ABNet ℓ	3	10	1.000 ± 0.000	0.024 ± 0.001	0.029 ± 0.003	0.027 ± 0.003
	EBP	2	10	—	0.001 ± 0.001	0.021 ± 0.004	0.026 ± 0.004
	BC	1	100	—	0.005 ± 0.001	0.015 ± 0.003	0.015 ± 0.003
	BNN	1	100	—	0.011 ± 0.002	0.023 ± 0.003	0.023 ± 0.003
mnist56	PBGNet	1	10	0.090 ± 0.001	0.023 ± 0.001	0.025 ± 0.003	0.024 ± 0.003
	ABNet	1	10	0.090 ± 0.001	0.023 ± 0.001	0.025 ± 0.003	0.024 ± 0.003
	PBGNet ℓ	1	50	0.974 ± 0.017	0.003 ± 0.001	0.008 ± 0.002	0.008 ± 0.003
	ABNet ℓ	1	10	1.000 ± 0.000	0.010 ± 0.002	0.017 ± 0.002	0.016 ± 0.002
	EBP	2	10	—	0.000 ± 0.000	0.019 ± 0.004	0.021 ± 0.005
	BC	3	50	—	0.004 ± 0.001	0.010 ± 0.003	0.010 ± 0.003
	BNN	1	100	—	0.004 ± 0.002	0.012 ± 0.001	0.012 ± 0.001
mnistLH	PBGNet	1	10	0.167 ± 0.010	0.058 ± 0.013	0.059 ± 0.010	0.060 ± 0.010
	ABNet	2	10	0.187 ± 0.003	0.087 ± 0.007	0.088 ± 0.006	0.087 ± 0.005
	PBGNet ℓ	1	100	0.998 ± 0.001	0.006 ± 0.001	0.022 ± 0.001	0.024 ± 0.002
	ABNet ℓ	3	10	0.895 ± 0.021	0.050 ± 0.005	0.060 ± 0.005	0.058 ± 0.006
	EBP	1	100	—	0.001 ± 0.000	0.027 ± 0.001	0.032 ± 0.002
	BC	1	100	—	0.013 ± 0.002	0.027 ± 0.001	0.027 ± 0.001
	BNN	1	100	—	0.023 ± 0.001	0.036 ± 0.001	0.036 ± 0.001

Table 4: Extended details on the selected architecture in the experiments on wide architectures: number of hidden layers ($L-1$), width (d), both C and KL divergence values from the computation of the corresponding bound, learning rate (LR) and epoch providing the best model (Best epoch) given the algorithm stops after 100 epochs.

Dataset	Model	$L-1$	d	KL	C	LR	Best epoch
ads	PBGNNet	3	10	26	0.45	0.01	64
	ABNet	2	10	29	0.47	0.01	51
	PBGNNet ℓ	3	10	66262	17.33	0.001	55
	ABNet ℓ	2	50	20940	14.50	0.01	52
adult	PBGNNet	1	10	238	0.30	0.1	87
	ABNet	1	10	233	0.30	0.1	77
	PBGNNet ℓ	2	10	3148	1.14	0.001	60
	ABNet ℓ	3	10	10014	1.93	0.01	52
mnist17	PBGNNet	1	10	181	1.39	0.1	96
	ABNet	1	10	171	1.35	0.1	78
	PBGNNet ℓ	2	10	425542	17.33	0.1	19
	ABNet ℓ	3	10	8578	6.66	0.01	33
mnist49	PBGNNet	1	10	342	0.93	0.1	95
	ABNet	1	10	329	0.91	0.1	86
	PBGNNet ℓ	1	50	39092	9.81	0.01	88
	ABNet ℓ	3	10	158982	17.33	0.1	57
mnist56	PBGNNet	1	10	202	0.95	0.01	87
	ABNet	1	10	196	0.93	0.1	97
	PBGNNet ℓ	1	50	35699	10.28	0.01	83
	ABNet ℓ	1	10	132207	17.33	0.1	82
mnistLH	PBGNNet	1	10	1386	0.74	0.1	93
	ABNet	2	10	1053	0.59	0.1	80
	PBGNNet ℓ	1	100	262046	10.97	0.01	90
	ABNet ℓ	3	10	81752	5.02	0.01	68